

Epoxide-Hydrolase-Initiated Hydrolysis/Rearrangement Cascade of a Methylene-Interrupted Bis-Epoxy Yields Chiral THF Moieties without Involvement of a "Cyclase"

Barbara T. Ueberbacher,^[a] Gustav Oberdorfer,^[b] Karl Gruber,^[b] and Kurt Faber*^[a]

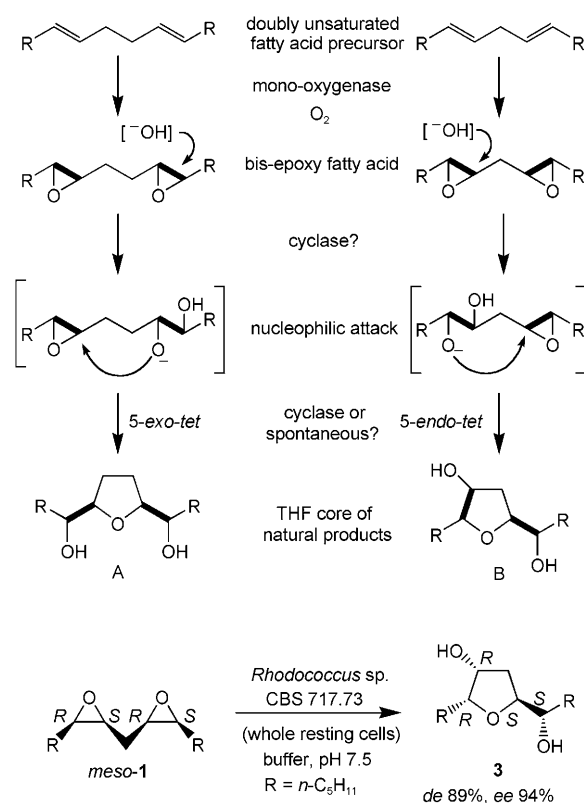
In contrast with electrophilic enzyme-catalysed cyclisations in terpenoid biosynthesis, cyclisations of tetrahydrofuran moieties found in several groups of natural products, such as annonaceous acetogenins, neurofurans and phytooxylipins, appear to proceed through a nucleophilic cascade mechanism starting from bis-epoxy fatty acid precursors. This hypothesis was verified by epoxide-hydrolase-catalysed hydrolytic ring-opening/cyclisation cascades starting from a methylene-interrupted

meso-bis-epoxide model substrate, which furnished the corresponding THF products with excellent *de* and *ee* values. Molecular modelling showed that the points of enzyme attack were consistent with the stereospecificities of the enzymes, whereas the stereochemical courses of the cyclisation were solely governed by Baldwin's rules and did not invoke the involvements of a "cyclase".

Introduction

Annonaceous acetogenins constitute a constantly growing group of natural products exclusively derived from tropical plants of the custard apple family (*Annonaceae* sp.).^[1] To date, more than 450 compounds of this class have been isolated and characterised, many of them possessing potent antileukaemic, cytotoxic, antihelminthic, antimalarial, antiprotozoal, pesticidal and immunosuppressant activities.^[2,3] Structurally, a typical annonaceous acetogenin is composed of a long aliphatic chain derived from a fatty acid, predominantly lacceroic (C-32) or ghedoic (C-34) acid, and bearing a unique α,β -unsaturated γ -lactone moiety at the carboxy terminus. The most intriguing common structural feature is the occurrence of (up to three) five- or six-membered cyclic ether units at the centre of the aliphatic chain. Since these show structurally recurring motifs, they are generally used for classification into subgroups. Approximately 85% of annonaceous acetogenins derived from the polyketide pathway^[4] contain either a mono- or bis-tetrahydrofuran (THF) motif, whereas epoxy, tris-THF and tetrahydropyran (THP) units occur only rarely.^[5]

The hypothesis that these compounds are formed from (poly)unsaturated fatty acids by enzymatic epoxidation of C=C moieties, leading to bis-epoxy fatty acids,^[6] has found support in the location of C=C bonds in the appropriate positions in the corresponding fatty acid chains^[7] and by identification of matching epoxidised fatty acid precursors (Scheme 1).^[8] These are bioactive themselves and are involved in the oxylipin pathway in plant defence pathways against pests and pathogens.^[9] The exact nature of the cyclisation step, however, still remains unclear, and the involvement of an isomerase/cyclase to form the THF core with the correct substitution pattern, including stereochemistry, has been a subject of speculation. As depicted in Scheme 1, it appears conceivable that the THF core systems A and B may be derived from ethylene- or methylene-interrupted bis-epoxides, respectively, through regio- and stereose-



Scheme 1. Presumed biosynthetic THF-formation pathway and whole cell biotransformation of *meso*-bis-epoxide 1.

[a] Dr. B. T. Ueberbacher, Dr. K. Faber
 Department of Chemistry, Organic and Bioorganic Chemistry,
 University of Graz, Heinrichstrasse 28, 8010 Graz (Austria)
 Fax: (+43) 316-380-9840
 E-mail: kurt.faber@uni-graz.at

[b] G. Oberdorfer, Dr. K. Gruber
 Institute of Molecular Biosciences,
 University of Graz, Humboldtstrasse 50/3, 8010 Graz (Austria)

lective enzyme-mediated nucleophilic attack by $[\text{OH}^-]$, which would trigger a spontaneous (or enzyme-mediated) ring-closure reaction.^[10]

Whereas annonaceous acetogenins (donnainin, for example) possess mostly THF cores of type A, type-B THF units occur in several types of natural products, such as neurofurans and phytooxylipins. Bioactive compounds incorporating this core have been isolated from marine organisms: ampezonol A, a polyhydroxy linear carbon-chain metabolite from *Amphidinium* sp., exhibits inhibitory activity against DNA polymerase α ,^[11] for example, whereas the THF diol from the brown alga *Notheia anomala* possesses potent nematocidal activity.^[12] Metabolites of different unsaturated fatty acids also possess THF core B. Linoleic acid derivatives with this structural motif found in corn cob show mitogenic activity,^[13] whereas THF metabolites of the neurofuran family derived from arachidonic and docosahexaenoic acids occur at elevated levels in the brain cortex in a mouse model of Alzheimer's disease.^[14]

It is noteworthy that in contrast with the majority of enzyme-catalysed cyclisations catalysed by cyclases/isomerases, which proceed through positively charged (carbenium ion) intermediates—generated by Lewis or Brønsted acid enzymatic catalysis,^[15]—these compounds would involve negatively charged (nucleophilic) alkoxy-species intermediates. In order to elucidate whether the cyclisation step is purely spontaneous—and consequently governed by Baldwin's rules,^[16]—or requires the involvement of an assisting isomerase/cyclase, we initiated the following study.

Results and Discussion

Prompted by the chance observation of an enzyme-triggered cascade reaction of haloalkyl-epoxides catalysed by whole bacterial cells,^[17] which yielded cyclisation products rather than hydrolysis products, we subjected the methylene-interrupted *meso*-bis-epoxide **1** as a model system to the presence of whole resting cells of *Rhodococcus* sp. CBS 717.73, and obtained the type-B THF product **3** in a highly stereoselective way (Scheme 1).^[18] Because the nature(s) of the enzyme(s) responsible for this whole-cell transformation remained obscure, we could only speculate as to whether the cascade was initiated by hydrolytic opening of an epoxy moiety catalysed by (unknown) epoxide hydrolases to yield an intermediate epoxy-diol, which underwent (enzyme-mediated or spontaneous) ring-closure to furnish the THF cyclisation product **3**. In a related fashion, cytosolic epoxide hydrolase from mammalian liver was shown to act on methylene-interrupted bis-epoxidised fatty acid esters to yield THF diols of type B at low enzyme concentrations, whereas tetrahydroxy products (derived from double hydrolysis of both epoxy moieties) were obtained at high enzyme loadings.^[19] In these studies, however, only the relative configurations of products were assigned and the exact stereochemical pathway—that is, the point of nucleophilic attack and the course of cyclisation—remained unclear.

During the past few years, an impressive range of epoxide hydrolases have been isolated and characterised in great detail.^[20] On the basis of their mechanisms of action, it has

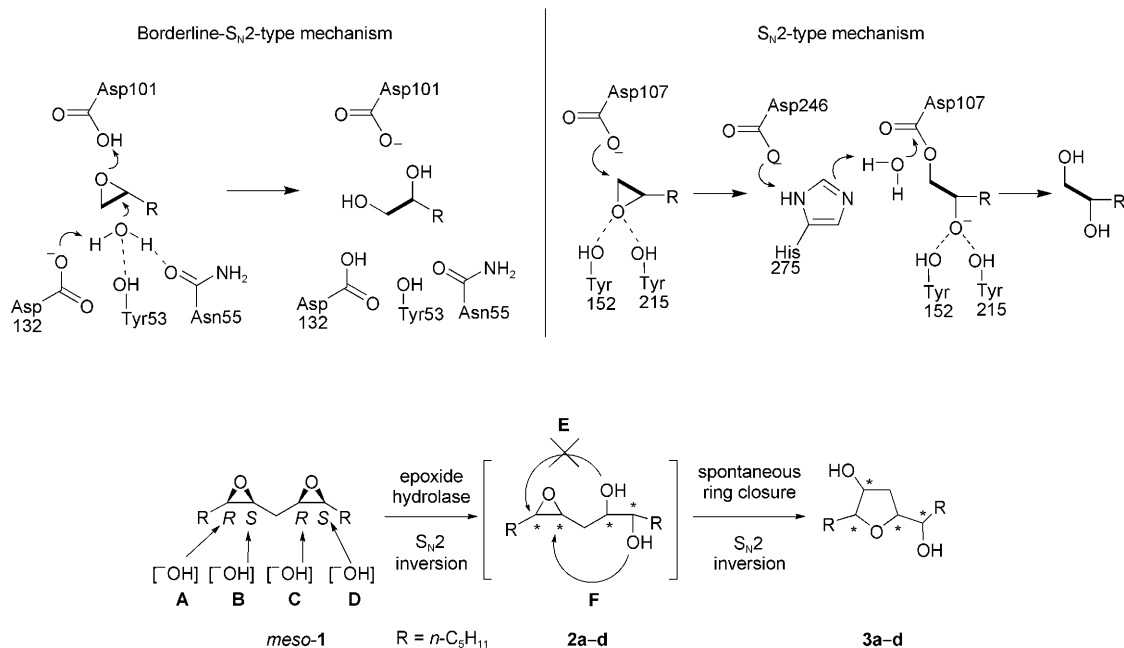
been shown that two distinct types of epoxide hydrolases exist that operate either through an S_N2 ^[21] or through a borderline S_N2 -type mechanism,^[22] both proceed with inversion of configuration at the attacked oxirane carbon atom. Because there are several available enzymes with structures that have been solved at high resolution, we anticipated that the regio- and stereoselective nucleophilic attack of $[\text{OH}^-]$ at a specific oxirane carbon atom of a bis-epoxide could be interpreted by molecular modelling. This enzyme-initiated step would lead to an activated (epoxy-diol) intermediate, which could undergo spontaneous or enzyme-mediated ring-closure. If the stereochemical outcome of the cyclisation product were to correspond to the stereochemistry of the epoxy-diol intermediate—determined by the point of nucleophilic attack as predicted by molecular modelling—no isomerase/cyclase would be required and the cyclisation would solely be governed by Baldwin's rules.^[16] Consequently, if the stereochemical course of the hydrolysis/cyclisation pathway were to deviate from the modelling prediction, the involvement of an isomerase/cyclase would be unavoidable.

Under the constraint that both steps in the hydrolysis/cyclisation cascade proceed with inversion of configuration,^[21,22] enzyme-catalysed nucleophilic attack at each of the four oxirane carbon atoms in the bis-epoxide **1** (Scheme 2 A–D) should in each case lead to a specific stereoisomer of the intermediate epoxy-diol (**2a–d**). Each of these could undergo cyclisation through pathways E or F to form cyclisation products **3**. Previously performed density functional theory calculations [PB-SCRF-B3LYP/6-311++g(d,p)//B3LYP/+6-31g(d)] had shown that pathway F for the spontaneous (nonenzymatic) cyclization reaction was favoured over pathway E by $\sim 3 \text{ kcal mol}^{-1}$.^[23] This is in agreement with Baldwin's rules of ring-closure, which predict that 5-*exo-tet* cyclisations (path F) are favoured whereas 6-*endo-tet* cyclisations (path E) are disfavoured.^[16]

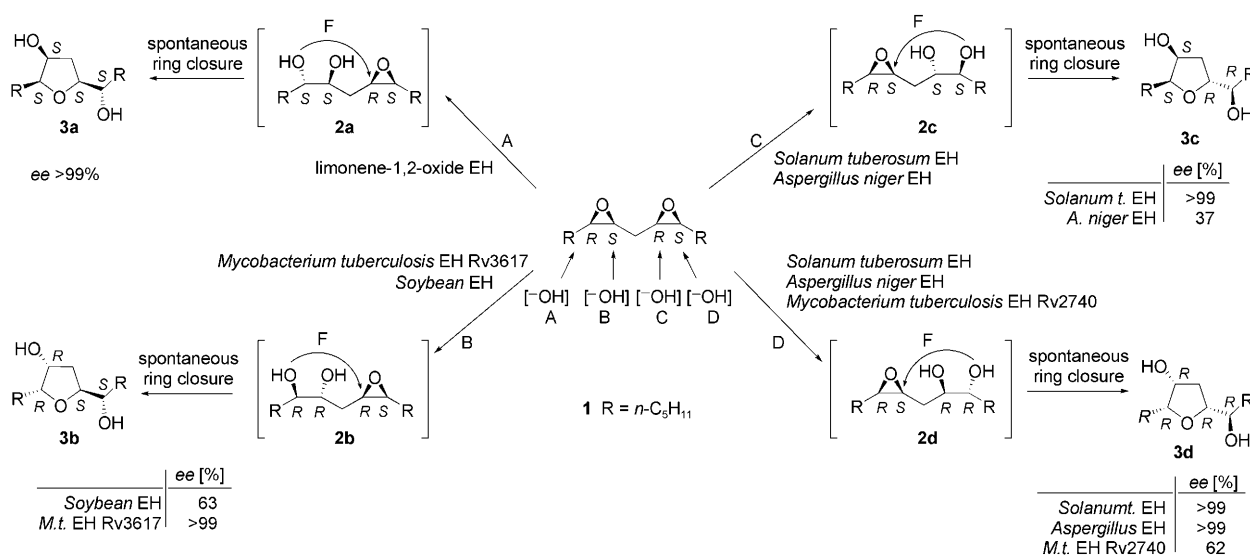
This hypothesis was tested with a range of cloned epoxide hydrolases of fungal (one), bacterial (eight) and plant (three) origin. For reason of comparison, seven mutants of soybean epoxide hydrolase were tested (Scheme 3, Table 1).

Overall, the majority of epoxide hydrolases were able to convert *meso*-bis-epoxide **1** at fair rates. Depending on the enzyme, three (**3a**, **3b** and **3d**) out of the four possible stereoisomers (**3a–3d**) of the expected THF derivatives were formed with varying stereoselectivities. The hydrolysis/cyclisation cascade proved to be remarkably "clean" and no tetrahydroxy products (which would originate from double hydrolysis of both epoxy moieties, as observed for bis-epoxidised fatty acids^[19]) could be detected. Cell-free extracts of "empty" *E. coli* host cells, which are devoid of epoxide hydrolases, were completely inactive. Likewise, intermediate epoxy-diols **2a–d** were not formed in measurable amounts.

The point of nucleophilic attack strongly depended on the type of enzyme. Whereas limonene-1,2-epoxide hydrolase attacked *meso*-bis-epoxide **1** at the "external" *R*-configured carbon atom (path A), epoxide hydrolases from *Glycine max* (soybean) and *Mycobacterium tuberculosis* Rv3617 preferred the "internal" *S*-configured carbon centre (path B). In a complementary fashion, epoxide hydrolases from *Solanum tuberosum*



Scheme 2. S_N2 and borderline- S_N2 mechanism of epoxide hydrolases, depicted for *Agrobacterium radiobacter* epoxide hydrolase and limonene epoxide hydrolase from *Rhodococcus erythropolis*, respectively. Stereochemical pathways for hydrolysis/cyclisation of **1** to form various stereoisomers of **3**, with possible sites of enzymatic nucleophilic attack (A–D) and cyclisation (E = 6-endo-*tet* disfavoured, F = 5-exo-*tet* favoured).



Scheme 3. Stereochemical courses of epoxide-hydrolase-catalysed hydrolysis/cyclization cascades of **1** to yield THF derivatives **3a–d**.

(potato), *Aspergillus niger* and *Mycobacterium tuberculosis* Rv2740 preferred the “external” *S*-configured carbon atom (path D). None of the enzymes showed a clear preference for path C.

Epoxide hydrolases from *Synechocystis radiodurans* and *M. tuberculosis* (Rv1938 and Rv2214c), as well as several enzyme mutants from *G. max*, showed activity towards bis-epoxide **1**, but did not display appreciable selectivities. Some epoxide hydrolases (from *Rhodococcus rhodochrous*, *Arabidopsis thaliana* and *Deinococcus radiodurans*) and the *G. max* H320Y mutant showed no activity.

Pathway A

Limonene-1,2-epoxide hydrolase (LEH) showed a preference for the “external” *R* and the “internal” *S*-configured carbon centres (pathways A and B, Scheme 3), the former being slightly favoured as indicated by the low *de* of 27%. Previous studies with this enzyme have shown that the nonnatural substrate cyclohexene oxide, which is also a *meso* compound, is hydrolysed to yield *rac-trans*-cyclohexane-1,2-diol;^[24] this indicates that LEH does not distinguish very well between adjacent carbon centres possessing opposite absolute configurations.^[25]

Table 1. Epoxide-hydrolase-catalysed hydrolysis/cyclisation cascades of *meso*-bis-epoxide **1**.

Epoxide hydrolase (EH)	<i>c</i> ^[a] [%]	<i>de</i> [%] ^[b] (3a + 3d)/(3b + 3c)	<i>ee</i> [%]			
			3a	3b	3c	3d
<i>G. max</i> EH (soybean)	71	−78	−	63	−	>99
limonene 1,2-epoxide EH (<i>Rhodococcus erythropolis</i>)	72	+27	>99	92	−	−
<i>S. tuberosum</i> EH	78	+69	−	−	>99	>99
<i>A. niger</i> EH	11	+83	−	−	37	>99
<i>M. tuberculosis</i> EH Rv 2740	25	+90	−	57	−	62
<i>M. tuberculosis</i> EH Rv 3617	89	−47	−	>99	−	27
<i>S. radiodurans</i> sp. EH PCC 6803	7	−33	−	29	−	18
<i>M. tuberculosis</i> EH Rv 1938	61	−9	63	40	−	−
<i>M. tuberculosis</i> EH Rv 2214c	4	+6	−	−	50	72
soybean EH mutant R156A	2	+8	−	4	−	>99
soybean EH mutant R205A	31	−33	−	40	−	>99
soybean EH mutant Y255S	24	−38	−	−	23	>99
soybean EH mutant D285C	15	−16	−	52	−	>99
soybean EH mutant D285E	5	−7	−	10	−	>99
soybean EH mutant Y175F	35	+76	−	−	76	>99
soybean EH mutant H320Y	<3	−	−	−	−	−
<i>R. rhodochrous</i> EH	<3	−	−	−	−	−
<i>A. thaliana</i> EH	<3	−	−	−	−	−
<i>D. radiodurans</i> EH	<3	−	−	−	−	−

[a] Conversion based on the sum of products formed versus remaining starting material after 24 h; [b] *de* of enantiomeric pairs **3a**+**3d** versus **3b**+**3c**; + diastereomer **3a**+**3d** in excess, − diastereomer **3b**+**3c** in excess.

Mechanistically, this may be explained by the unusual “push–pull” borderline-S_N2 mechanism of this enzyme, in which the epoxide moiety is activated through O-protonation by an aspartate residue (D101) with simultaneous nucleophilic attack by a water molecule which is formally deprotonated by a second aspartate residue (D132; Scheme 2).

Pathway B

Hydrolysis of *meso*-**1** with *G. max* (soybean) EH preferentially took place at the *S*-configured carbon atoms, with preference for the “internal” (path B) over the “external” carbon atom (path C); this is in line with previous studies in which the natural substrate (*cis*-9,10-epoxystearic acid) was attacked at the *S*-configured centre, but with relaxed regioselectivity, with both the 9*R*,10*S* and 9*S*,10*R* enantiomers, yielding (9*R*,10*R*)-dihydroxystearic acid as the sole product.^[26] With linoleic acid monoepoxides the picture is very similar. Soybean EH catalysed the hydrolysis of (12*Z*)-9,10-epoxyoctadec-12-enoic and (9*Z*)-12,13-epoxyoctadec-9-enoic acids to the corresponding (9*R*,10*R*)- and (12*R*,13*R*)-dihydroxyacids with high enantiomeric excess by attack at the *S* centres.^[27] Epoxide hydrolase Rv3617 from *M. tuberculosis* showed the same—although less pronounced—preference as *G. max* EH.

Pathway C

None of the enzymes were able to catalyse pathway C efficiently; only *A. niger* and *S. tuberosum* EH produced stereoisomer **3c** in minor amounts as a side reaction from pathway D (see below).

Pathway D

S. tuberosum EH and *A. niger* EH both show preference for the “external” *S*-configured carbon atom (path D) going hand in hand with attack at the “internal” *R*-configured centre to form **3c** by pathway C. This behaviour is in line with the observation that *S. tuberosum* EH (like *G. max* EH) shows high specificity towards the *S*-configured centre in *cis*-9,10-epoxystearic acid.^[26] *M. tuberculosis* EH Rv2740—the second enzyme so far known to act by a borderline-S_N2 mechanism similar to that of limonene 1,2-epoxide EH,^[28]—also preferentially attacked the “external” *S*-configured carbon (path D) with high regioselectivity. In contrast, side product **3b** (originating from attack at the “internal” *S* configured centre) was formed only in minor amounts (5%).

Molecular modelling

To explain the stereospecificities observed in the hydrolysis of *meso*-bis-epoxide **1** in the presence of epoxide hydrolases we performed molecular docking calculations on all the enzymes for which structures were available: that is, limonene-1,2-epoxide hydrolase,^[22] as well as the epoxide hydrolases from *M. tuberculosis*,^[28] *A. niger*,^[21] and *S. tuberosum*.^[29] Initial docking runs were conducted with a modified substrate in which the terminal *n*-pentyl groups were replaced by ethyl substituents. This simplified model substrate has fewer degrees of freedom, making it computationally easier to handle, especially in rigid enzyme active sites. The resulting binding modes were further subjected to geometry optimization by molecular mechanics. We had previously been able to show that the best-scored structures from docking calculations are not necessarily those with the lowest energies after energy minimization.^[30] We therefore used the lowest-energy complex structures after geometry optimization for our analysis.

We were pleased to see that in the case of limonene-1,2-epoxide hydrolase, our modelling results were clearly in line with the experimentally observed parallel attack at the “external” *R* and the “internal” *S*-configured carbon centres (pathways A and B, respectively). The identification of the preferred carbon atom, however, is less straightforward. In the modelled complex structures, the distances from the attacking water molecule to the “external” *R* and the “internal” *S*-configured carbon atom are very similar (3.0 versus 3.2 Å). If the angles between the nucleophile and the oxirane carbon atoms are taken into account, however, a more favourable geometry for the trajec-

tory of attack on the “external” carbon atom than for the “internal” carbon atom (81.9° in pathway A versus 70.5° in pathway B, Figure 1) would be consistent with the experimental results, which show a slight preference for path A.

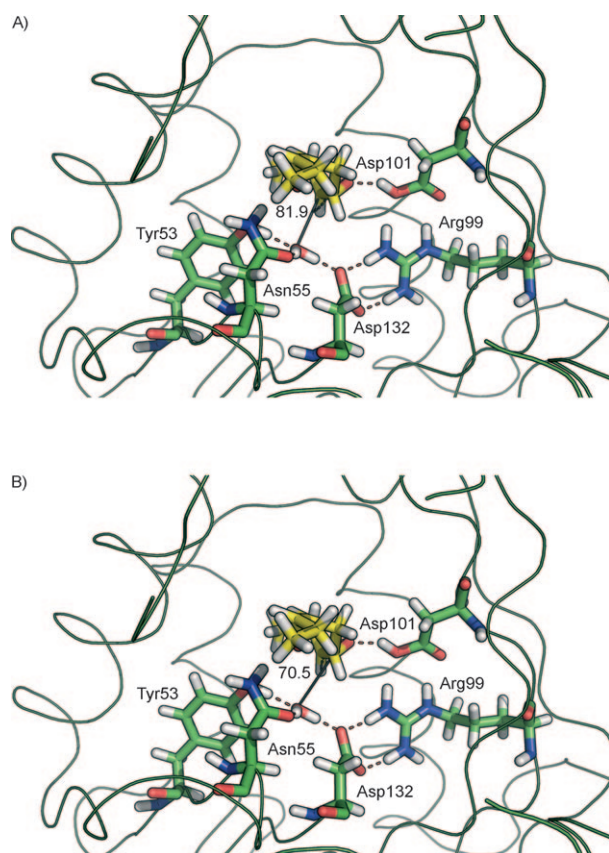


Figure 1. Docked and optimized enzyme–substrate complex of limonene-1,2-epoxide hydrolase (green) and ethyl-substituted bis-epoxide (yellow). Essential amino acid residues in active site are labelled, hydrogen bonding interactions are indicated as red dashes, and the trajectory of nucleophilic attack of water is indicated as a grey stick including the angle of approach [°] to the oxirane carbon atom: A) shows pathway A, B) shows pathway B (picture generated with PyMol, <http://www.pymol.org/>).

The structure of the epoxide hydrolase from *M. tuberculosis* differs somewhat from that of limonene-1,2-epoxide hydrolase, although both enzymes act through the same push-pull borderline- S_N2 mechanism. In the latter enzyme, the C-terminal α helix is shorter and folds back into the active site. Therefore, the active site of the *Mycobacterium* enzyme is wider and more space is available for solvent and substrate (Figure 2). A structural superposition involving only essential catalytic residues, however, showed an root mean square deviation of 1.6 Å; this indicates very similar active site geometries.

Again, the modelling results are in line with the experimental results: the wider active site and the increased accessibility allow the reduced stereospecificities observed for the *Mycobacterium* enzyme to be explained (*ee* = 62%). The carbon atom most likely to be attacked by the water molecule indicated a preference for pathway D (Figure 3).

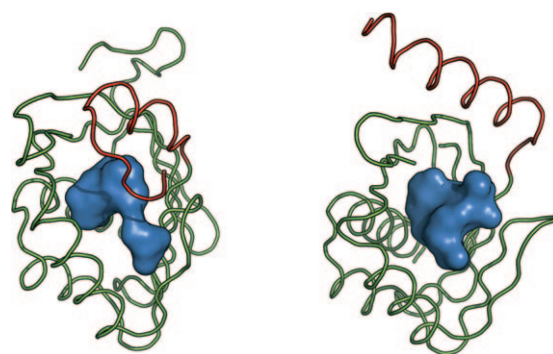


Figure 2. A) Ribbon representations of A) limonene-1,2-epoxide hydrolase and B) the EH from *Mycobacterium tuberculosis* (right). The C-terminal α helices are shown in red. The blue blobs represent the shapes and sizes of the active site cavities.

In the case of the epoxide hydrolases from *A. niger* and from *S. tuberosum*, which act through S_N2 mechanisms, neither molecular docking simulations nor the subsequent geometry optimizations yielded productive binding modes for the simplified bis-epoxide substrate (that is, with the catalytic aspartate residue—as nucleophile—close to one of the oxirane rings). A more qualitative comparison of the active sites of both enzymes showed that the active site of the *Solanum* enzyme is significantly bigger and forms a deep and wide channel into the interior of the protein (Figure 4). This structural difference might also explain the observed small differences in the stereoselectivities of these enzymes.

Conclusions

Epoxide hydrolases from various sources (plants, bacteria and fungi) were found to catalyse transformations of the *meso*-bis-epoxide **1** by hydrolysis/cyclisation cascades to furnish the THF derivatives **3a**, **3b** and **3d**. Analysis of the stereochemical courses of the cascades by molecular modelling revealed that the hydrolytic initiation of the cascade was solely determined by the stereopreferences of the enzymes, whereas the cyclisations of the intermediate epoxy-diols were governed by Baldwin's rules. Our results show that the reaction pathway is 1) initiated by epoxide-hydrolase-catalysed hydrolysis of an oxirane moiety, followed by 2) spontaneous ring-closure of the epoxy-diol intermediate. Consequently, no involvement of a “cyclase” is required for this type of cascade cyclisation.

Experimental Section

General: NMR spectra were recorded in $CDCl_3$ with a Bruker Amx 360 instrument at 360 MHz (1H) and 90 MHz (^{13}C). Chemical shifts are reported relative to TMS (δ = 0.00 ppm) with $CHCl_3$ as internal standard; coupling constants (*J*) are given in Hz. TLC was performed on Merck 60 silica gel (F_{254}) and compounds were visualised by dipping into Mo-containing reagent $[(NH_4)_6Mo_7O_{24} \cdot 4H_2O]$ (100 g L $^{-1}$) and $Ce(SO_4)_2$ in H_2SO_4 (10%). Compounds were

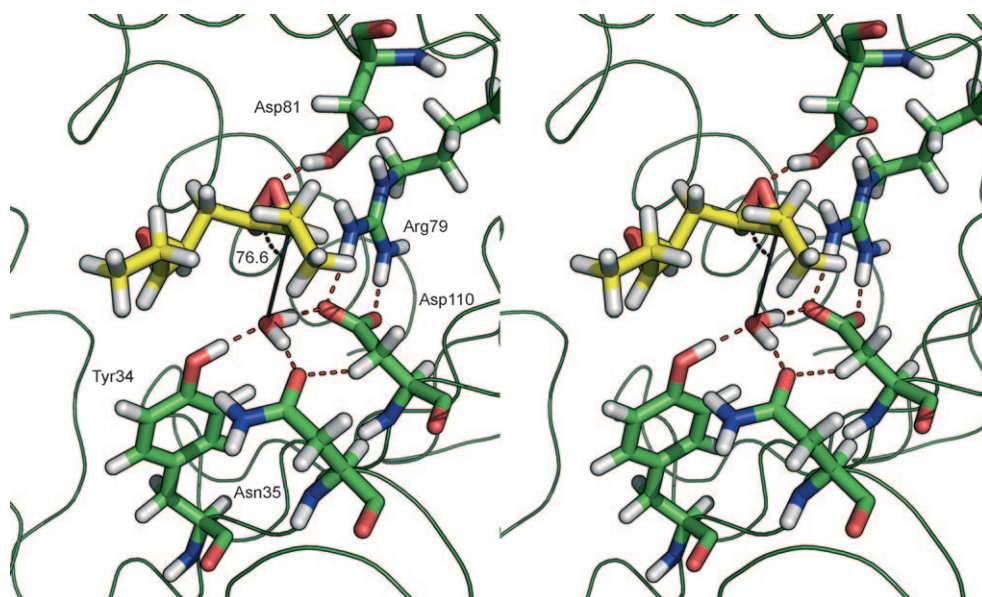


Figure 3. Stereorepresentation of the final docked and energy-minimized enzyme-substrate complex of *Mycobacterium tuberculosis* EH with ethyl-substituted bis-epoxide. Essential amino acid residues in the active site are labelled, hydrogen bonding interactions are indicated as red dashes, and the trajectory of nucleophilic attack of water is indicated as a grey stick including the angle of approach [76.6°] to the oxirane carbon atom and indicating pathway D (picture generated with PyMol, <http://www.pymol.org/>).

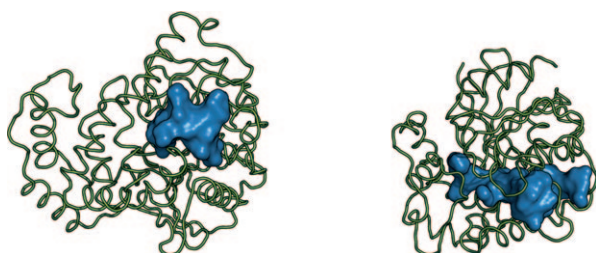


Figure 4. Ribbon representation of epoxide hydrolases from A) *Aspergillus niger* and B) *Solanum tuberosum*, that show large differences in the shapes and sizes of the active site architectures (picture generated with PyMol, <http://www.pymol.org/>).

purified by flash chromatography on silica gel (Merck 60, 230–400 mesh). The petroleum ether used had a boiling range of 60–90 °C.

Synthesis of substrates: (6*R**,7*S**,9*R**,10*S**)-6,7:9,10-Bis(epoxy)-pentadecane (**1**) and the reference materials—the enantiomeric (6*R**,7*R**,9*S**,10*S**)-6,9-epoxypentadecane-7,10-diols **3b** and **3c** and (6*R**,7*R**,9*R**,10*R**)-6,9-epoxypentadecane-7,10-diols **3a** and **3d**—were synthesised as previously described.^[18] NMR data were consistent with the literature.^[18]

Enzymes: Cloned *G. max* EH and mutants thereof were obtained from Elisabeth Blee (Strasbourg, France). Cell-free extracts of over-expressed limonene-1,2-epoxide hydrolase and epoxide hydrolases from *S. tuberosum*, *R. erythropolis*, *D. radiodurans*, *Synechocystis* sp. PCC 6803 and *M. tuberculosis* Rv1938, Rv3617, Rv2214c and Rv2740 were provided by Michael Arand (Zürich, Switzerland); purified *Ara-bidopsis thaliana* epoxide hydrolase was provided by Johan Meijer (Uppsala, Sweden). Epoxide hydrolase preparations from *A. niger* and *R. rhodochrous* were purchased from Fluka.

Biotransformations

General procedure for the enzymatic hydrolysis of (6*R,7*S**,9*R**,10*S**)-6,7:9,10-bis-epoxy-pentadecane (**1**):** Lyophilised cells (20 mg, in cases of cell-free extracts and enzyme preparations 5 mg) were rehydrated in Tris-HCl buffer (1 mL, 0.05 M, pH 8) for 1 h at 30 °C and 130 rpm. After addition of substrate **1** (5 µL) the mixture was agitated for 24 h at 30 °C and 130 rpm. The reactions were stopped by extraction with CH₂Cl₂ (500 µL). The organic layer was dried over Na₂SO₄ and analysed. For chiral analyses, *N*-methyl-bis(trifluoroacetamide) (40 µL) was added and the mixture was stirred for 1 h at room temperature. After quenching with water and drying over Na₂SO₄, samples were analysed by GC.

Analytical methods: GC analyses were carried out on a Varian3800 gas chromatograph equipped with flame ionisation detection (FID) and a CP1301 capillary column (column A, 30 m, 0.25 mm). Enantiomeric purities were analysed

with the aid of an Astec ChiralDEX B-TA column (column B, 30 m, 0.25 mm; Whippany, NJ, USA). H₂ was used as the carrier gas. Chiral materials were analysed as the corresponding trifluoroacetate esters. For analytical data see Tables 2 and 3.

Table 2. GC data on an achiral stationary phase.

Compound	Column ^[a,b]	<i>t_R</i> [min]
(6 <i>R</i> *,7 <i>S</i> *,9 <i>R</i> *,10 <i>S</i> *)-6,7:9,10-bis(epoxy)pentadecane (1)	A	9.52
(6 <i>R</i> *,7 <i>R</i> *,9 <i>S</i> *,10 <i>S</i> *)-6,9-epoxypentadecane-7,10-diols 3b and 3c	A	11.79
(6 <i>R</i> *,7 <i>R</i> *,9 <i>R</i> *,10 <i>R</i> *)-6,9-epoxypentadecane-7,10-diols 3a and 3d	A	11.49

[a] Column A: CP1301 capillary column. [b] Method: 69 kPa N₂; hold at 200 °C for 5 min; heat rate 5 °C min⁻¹ to 250 °C; hold at 250 °C for 10 min.

Docking and molecular mechanics calculations: Molecular models of the ethyl-simplified bis-epoxide (cf. Scheme 1, *meso*-**1**, R = Et) were built with Sybyl v7.3 (<http://www.tripos.com>) and optimized by use of the Tripos force field. Partial charges for the model substrates were computed with the Antechamber program of Amber 9.0 by the semiempirical AM1-bcc method.^[31]

3D-coordinates of the epoxide hydrolase structures were taken from the PDB (IDs: 1nu3, 2bng, 2cjp and 1qo7) and were prepared according to the requirements of AutoDock v4.0 (addition of polar hydrogen atoms, addition of partial charges, assignation of atom types) by use of the provided python scripts.

Because the four EHs exhibit two different reaction mechanism types, slightly different docking strategies were chosen. In the case

Table 3. GC data on a chiral stationary phase.

Compound ^[a]	Column ^[b,c]	t _R [min]
(6R*,7S*,9R*,10S*)-6,7:9,10-bis(epoxy)pentadecane (1)	B	9.63
(6S,7S,9S,10S)-6,9-epoxypentadecane-7,10-diol (3a)	B	17.54
(6R,7R,9S,10S)-6,9-epoxypentadecane-7,10-diol (3b)	B	22.24
(6S,7S,9R,10R)-6,9-epoxypentadecane-7,10-diol (3c)	B	21.97
(6R,7R,9R,10R)-6,9-epoxypentadecane-7,10-diol (3d)	B	18.11

[a] Measured as bis-trifluoroacetate esters. [b] Column B: Astec Chiral-dex B-TA column. [c] Method: 55 kPa H₂; hold at 155 °C for 25 min; heat rate 10 °C min⁻¹ to 180 °C; hold at 180 °C for 10 min.

of limonene-1,2-epoxide hydrolase and the epoxide hydrolase from *M. tuberculosis* (borderline-S_N2 mechanism) a water molecule, which is believed to be the essential nucleophile for oxirane attack and is present in both crystal structures (hydrogen-bonded to conserved tyrosine, aspartate and asparagine residues), was retained and modelled with a van der Waals radius of 1.4 Å, but without partial charges. In contrast, catalysis by the S_N2-type epoxide hydrolases from *A. niger* and *S. tuberosum* involves a covalent "glycol-monoester-enzyme" intermediate with the substrate bound onto an aspartate residue. Because covalent docking turned out to be difficult with the available software, we decided to generate docking poses mimicking Michaelis complexes before the substrate is actually attacked by the aspartate nucleophile of the enzyme.

Docking calculations were performed with AutoDock v4.0^[32] with use of the implemented Lamarckian genetic algorithm with a population size of 150 individuals, and an average number of generations of about 200. In each case, the cubic energy grid was centred on the carboxylate group of the essential active site aspartate residue in each protein, extending 22.5 Å in each direction. The ligand was fully flexible, whereas the protein was kept rigid during docking runs. Every calculation consisted of ten independent docking runs, after which the resulting binding modes were clustered with an root mean square deviation of 1.5 Å.

Molecular mechanics calculations were carried out with the aid of programs from the AMBER 9.0 suite.^[31] Energy minimization was performed in vacuo with a distance-dependent dielectric function for all complex structures obtained in the docking simulations with use of the *gaff* force field for the ligands and the *ff03* force field for the protein. All atoms beyond a sphere of 16 Å from the centre of the docking grid were restrained to their original positions. The minimizations were run for a maximum of 5000 cycles.

Acknowledgements

Financial support by the Austrian Science Fund (FWF, Vienna, W9 DK Molecular Enzymology) is gratefully acknowledged. We thank E. Blee (Strasbourg) for providing G. max epoxide hydrolase and mutants thereof, M. Arand (Zürich) for providing limonene 1,2-epoxide hydrolase from *R. erythropolis* and epoxide hydrolases from *S. tuberosum*, D. radiodurans, *Synechocystis* sp. and *M. tuberculosis*, and J. Meijer (Uppsala) for the donation of epoxide hydrolase from *Arabidopsis thaliana*.

Keywords: bis-epoxides • cascade reactions • enzyme models • epoxide hydrolases • hydrolases

- [1] A. Cave, B. Figadere, A. Laurens, D. Cortes, *Prog. Chem. Org. Nat. Prod.* **1997**, 70, 81–288; J. K. Rupprecht, Y.-H. Hui, J. L. McLaughlin, *J. Nat. Prod.* **1990**, 53, 237–278; X.-P. Fang, M. J. Rieser, Z.-M. Gu, G.-X. Zhao, J. L. McLaughlin, *Phytochem. Anal.* **1993**, 4, 27–48; F. Q. Alali, X.-X. Liu, J. L. McLaughlin, *J. Nat. Prod.* **1999**, 62, 504–540.
- [2] M. C. Zafra-Polo, M. C. Gonzalez, E. Estornell, S. Sahpaz, D. Cortes, *Phytochemistry* **1996**, 42, 253–271.
- [3] The antileukemic agent uvaricin was discovered as the first representative in 1982; see M. S. Tempesta, G. R. Kriek, R. B. Bates, *J. Org. Chem.* **1982**, 47, 3151–3153.
- [4] A. R. Gallimore, C. B. W. Stark, A. Bhatt, B. M. Harvey, Y. Demydchuk, V. Bolanos-Garcia, D. J. Fowler, J. Staunton, P. F. Leadlay, J. B. Spencer, *Chem. Biol.* **2006**, 13, 453–460; A. R. Gallimore, J. B. Spencer, *Angew. Chem.* **2006**, 118, 4514–4521; *Angew. Chem. Int. Ed.* **2006**, 45, 4406–4413; for a stereochemical model of polyether antibiotics see: D. E. Cane, W. D. Celmer, J. W. Westley, *J. Am. Chem. Soc.* **1983**, 105, 3594–3600.
- [5] A. Bermejo, B. Figadere, M.-C. Zafra-Polo, I. Barrachina, E. Estornell, D. Cortes, *Nat. Prod. Rep.* **2005**, 22, 269–303; M. C. Zafra-Polo, B. Figadere, T. Gallardo, J. R. Tormo, D. Cortes, *Phytochemistry* **1998**, 48, 1087–1117.
- [6] D. O'Hagan, *Nat. Prod. Rep.* **1989**, 6, 205–219.
- [7] C. Gleye, S. Raynaud, R. Hocquemiller, A. Laurens, C. Fourneau, L. Serani, O. Laprevote, F. Roblot, M. Leboeuf, A. Fournet, A. R. De Arias, B. Figadere, A. Cave, *Phytochemistry* **1998**, 47, 749–754.
- [8] L. Zeng, Q. Ye, N. H. Oberlies, G. Shi, Z. M. Gu, K. He, J. L. McLaughlin, *Nat. Prod. Rep.* **1996**, 13, 275–306; Z. M. Gu, G. X. Zhao, N. H. Oberlies, L. Zeng, J. L. Laughlin, in: *Recent Advances in Phytochemistry*, Vol. 29, Plenum, New York, **1995**, pp. 249–310; C. Gleye, S. Raynaud, C. Fourneau, A. Laurens, O. Laprevote, L. Serani, A. Fournet, R. Hocquemiller, *J. Nat. Prod.* **2000**, 63, 1192–1196; C. Gleye, A. Laurens, O. Laprevote, L. Serani, R. Hocquemiller, *Phytochemistry* **1999**, 52, 1403–1408.
- [9] I. Prost, S. Dhont, G. Rothe, J. Vicente, M. J. Rodriguez, N. Kift, F. Carbone, G. Griffiths, M.-T. Esquerre-Tugay, S. Rosahl, C. Castresana, M. Hamberg, J. Fournier, *Plant Physiol.* **2005**, 139, 1902–1913; E. Blee, *Prog. Lipid Res.* **1998**, 37, 33–72.
- [10] Y. Hu, A. R. L. Cecil, X. Frank, C. Gleye, B. Figadere, R. C. D. Brown, *Org. Biomol. Chem.* **2006**, 4, 1217–1219.
- [11] T. Kubota, Y. Sakuma, K. Shimbo, M. Tsuda, M. Nakano, Y. Uozumi, J. Kobayashi, *Tetrahedron Lett.* **2006**, 47, 4369–4371.
- [12] R. J. Capon, R. A. Barrow, S. Rochfort, M. Jobling, C. Skene, E. Lacey, J. H. Gill, T. Friedel, D. Wadsworth, *Tetrahedron* **1998**, 54, 2227–2242.
- [13] B. M. Markaverich, M. A. Alejandro, D. Markaverich, L. Zitzow, N. Casajuna, N. Camarao, J. Hill, K. Bhirdo, R. Faith, J. Turk, J. R. Crowley, *Biochem. Biophys. Res. Commun.* **2002**, 291, 692–700.
- [14] W.-L. Song, J. A. Lawson, D. Reilly, J. Rokach, C.-T. Chang, B. Giasson, G. A. FitzGerald, *J. Biol. Chem.* **2008**, 283, 6–16.
- [15] The largest and best-described group of cyclases (terpenoid cyclases) uses either a Lewis-acid-catalysed (Mg^{II}, Type I cyclases) activation of an allylic diphosphate precursor or the Brønsted-acid-mediated (Asp, I cyclases) electrophilic activation of an olefin or an epoxide. The initiation step creates a carbenium ion, which is immediately trapped by an adjacent alkene, and generates the next carbenium ion, and so forth. Finally, this electrophilic cascade is terminated either by deprotonation (or by hydration) of the last carbenium ion to furnish an alkene (or an alcohol) as the final product of the cyclisation cascade. For reviews see: D. W. Christianson, *Chem. Rev.* **2006**, 106, 3412–3442; K. U. Wendt, G. E. Schultz, E. J. Corey, D. R. Liu, *Angew. Chem.* **2000**, 112, 2930–2952; *Angew. Chem. Int. Ed.* **2000**, 39, 2812–2833.
- [16] J. E. Baldwin, *J. Chem. Soc. Chem. Commun.* **1976**, 734–738. Although enzymes obey the Baldwin rules in general, exceptional anti-Baldwin- or anti-Markovnikov cyclisations are known; cf. ref. [15] and J. A. Piccirilli, *Chem. Biol.* **1999**, 6, R59–R64. Recently, the first enzymes that disobey Baldwin's rules were found in the biosynthesis of the polyether antibiotic lasalocid. LasB/Lsd19 epoxide hydrolases catalyse the ring-closure of a bis-epoxy-alcohol precursor through a disfavoured 6-*endo-tet* cyclisation, instead of the favoured 5-*exo-tet* cyclisation, see: Y. Shichijo, A. Migita, H. Oguri, M. Watanabe, T. Tokiwano, K. Watanabe, H. Oikawa, *J. Am. Chem. Soc.* **2008**, 130, 12230–12231; L. Smith, H. Hong, J. B. Spencer, P. F. Leadlay, *ChemBioChem* **2008**, 9, 2967–2975.

- [17] S. F. Mayer, A. Steinreiber, R. V. A. Orru, K. Faber, *Eur. J. Org. Chem.* **2001**, 4537–4542; for a review on enzyme-initiated cascade-reactions see: S. F. Mayer, W. Kroutil, K. Faber, *Chem. Soc. Rev.* **2001**, 30, 332–339.
- [18] S. M. Glueck, W. M. F. Fabian, K. Faber, S. F. Mayer, *Chem. Eur. J.* **2004**, 10, 3467–3478.
- [19] P. P. Halarnkar, J. Nourooz-Zadeh, E. Kuwano, A. D. Jones, B. D. Hammock, *Arch. Biochem. Biophys.* **1992**, 294, 586–593; P. P. Halarnkar, R. N. Wixtrom, M. H. Silva, B. D. Hammock, *Arch. Biochem. Biophys.* **1989**, 272, 226–236; B. Borhan, J. Nourooz-Zadeh, T. Uematsu, B. D. Hammock, M. J. Kurth, *Tetrahedron* **1993**, 49, 2601–2612; J. Nourooz-Zadeh, T. Uematsu, B. Borhan, M. J. Kurth, B. D. Hammock, *Arch. Biochem. Biophys.* **1992**, 294, 675–685.
- [20] M. Arand, A. Cronin, M. Adamska, F. Oesch, *Methods Enzymol.* **2005**, 400, 569–588; C. A. G. M. Weijers, J. A. M. de Bont, *J. Mol. Catal. B* **1999**, 6, 199–214.
- [21] For the epoxide hydrolase from *Agrobacterium radiobacter* see: M. Nardini, R. Rink, D. B. Janssen, B. W. Dijkstra, *J. Mol. Catal. B* **2001**, 11, 1035–1042; M. Nardini, I. S. Ridder, H. J. Rozeboom, K. H. Kalk, R. Rink, D. B. Janssen, B. W. Dijkstra, *J. Biol. Chem.* **1999**, 274, 14579–14586; for the epoxide hydrolase from *A. niger* see: J. Zou, B. M. Hallberg, T. Bergfors, F. Oesch, M. Arand, S. L. Mowbray, T. A. Jones, *Structure* **2000**, 8, 111–122.
- [22] For limonene 1,2-epoxide hydrolase from *Rhododoccus erythropolis* see: M. Arand, B. M. Hallberg, J. Zou, T. Bergfors, F. Oesch, M. J. van der Werf, J. A. M. de Bont, T. A. Jones, S. L. Mowbray, *EMBO J.* **2003**, 22, 2583–2592.
- [23] Although the Gibbs free energies (ΔG_{react}) for both cyclisation pathways were $\sim 17 \text{ kcal mol}^{-1}$, a significant energetic discrimination of $\sim 3 \text{ kcal mol}^{-1}$ was found between deprotonation energies of alcohol groups of epoxy-diol intermediates, thereby favouring pathway F over E, which (translated into kinetic terms) is $> 99\%$; see ref. [18].
- [24] M. J. van der Werf, R. V. A. Orru, K. M. Overkamp, H. J. Swarts, I. Osprian, A. Steinreiber, J. A. M. de Bont, K. Faber, *Appl. Microbiol. Biotechnol.* **1999**, 52, 380–385.
- [25] Likewise, LEH was shown to hydrolyse both enantiomers of its natural substrate (limonene-1,2-epoxide) in an enantioconvergent fashion through opposite regioselective nucleophilic attack; see ref. [24].
- [26] E. Blee, F. Schubert, *J. Biol. Chem.* **1992**, 267, 11 881–11 887; S. Summerer, A. Hanano, S. Utsumi, M. Arand, F. Schubert, E. Blee, *Biochem. J.* **2002**, 366, 471–480.
- [27] E. Blee, F. Schubert, *Eur. J. Biochem.* **1995**, 230, 229–234.
- [28] P. Johansson, T. Unge, A. Cronin, M. Arand, T. Bergfors, T. A. Jones, S. L. Mowbray, *J. Mol. Biol.* **2005**, 351, 1048–1056.
- [29] S. L. Mowbray, L. T. Elfström, K. M. Ahlgren, C. E. Andersson, M. Widestén, *Protein Sci.* **2006**, 15, 1628–1637.
- [30] G. Oberdorfer, C. Stueckler, M. Hall, K. Faber, K. Gruber in *Flavins and Flavoproteins* (Eds.: S. Frago, C. Gomez-Moreno, M. Medina), Prensas Universitarias de Zaragoza, Zaragoza, **2008**, pp. 553–558.
- [31] D. A. Case, T. A. Darden, T. E. Cheatham, III, C. L. Simmerling, J. Wang, R. E. Duke, R. Luo, K. M. Merz, D. A. Pearlman, M. Crowley, R. C. Walker, W. Zhang, B. Wang, S. Hayik, A. Roitberg, G. Seabra, K. F. Wong, F. Paesani, X. Wu, S. Brozell, V. Tsui, H. Gohlke, L. Yang, C. Tan, J. Mongan, V. Hornak, G. Cui, P. Beroza, D. H. Mathews, C. Schafmeister, W. S. Ross, P. A. Kollman, AMBER 9, University of California, San Francisco, **2006**.
- [32] R. Huey, G. M. Morris, A. J. Olson, D. S. Goodsell, *J. Comput. Chem.* **2007**, 28, 1145–1152.

Received: March 25, 2009

Published online on June 3, 2009